Neuropsychiatric Disease and Treatment

Dovepress

open access to scientific and medical research

Open Access Full Text Article

ORIGINAL RESEARCH

lncRNA-Associated Competitive Endogenous RNA Regulatory Network in an $A\beta_{25-35}$-Induced AD Mouse Model Treated with Tripterygium Glycoside

Liang Tang[1–4]
Qin Xiang[1–4]
Ju Xiang[1–4]
Jianming Li[1–5]

[1]Department of Basic Biology, Changsha Medical College, Changsha, People's Republic of China; [2]Department of Basic Biology, Wuzhou Medical College, Wuzhou, People's Republic of China; [3]Center for Neuroscience and Behavior, Changsha Medical College, Changsha, People's Republic of China; [4]Academics Working Station, Changsha Medical College, Changsha, People's Republic of China; [5]Department of Rehabilitation, Xiangya Boai Rehabilitation Hospital, Changsha, 410100, People's Republic of China

Background: Tripterygium glycoside (TG) has been suggested to have protective effects on the diseases of the central nervous system including Alzheimer's disease (AD). The mechanisms involving lncRNA-associated competing endogenous RNAs (ceRNAs) were shown to play important roles in the development of AD. However, the ceRNA mechanism of TG in treating AD is still unknown. Thus, we aimed to explore the ceRNA mechanism in the treatment of AD with TG.

Methods: A total of 32 C57BL/6J mice were administered 3 μL of $A\beta_{25-35}$ (dual side, 1 mg/mL) by a single stereotactic injection in the brain to conduct AD mouse model. AD mouse models were randomly selected and divided into the AD+normal saline (NS) group (n=16) and the AD+TG group (n=16). The expression data of lncRNAs, mRNAs, and miRNAs in the hippocampus of mice from AD+NS group (n=3) and the AD+TG group (n=3) were obtained by microarray analysis. The MuTaME method was used to predict the ceRNA regulatory network. Gene ontology (GO) and Kyoto Encyclopedia of Genes and Genomes (KEGG) analyses were performed using the DAVID database. A protein–protein interaction (PPI) network was constructed by using STRING software.

Results: TG can significantly improve spatial memory and inhibit the production of p-tau in an $A\beta_{25-35}$-induced AD mouse model. A total of 661 differentially expressed lncRNAs, 503 mRNAs, and 13 miRNAs were identified. A ceRNA network involving the top 200 mRNA-miRNA-lncRNA pairs with 16 lncRNAs, 11 miRNAs, and 52 mRNAs was visualized. And a PPI network complex filtered 26 gene nodes in DEGs was predicted.

Conclusion: We have identified 503 DEGs, 661 DElncRNAs, and 13 DEmiRNAs during treatment with TG in $A\beta_{25-35}$-induced AD mouse model. A ceRNA network based on the DElncRNAs, DEmRNAs, and DEmiRNAs was conducted, which provided new insight into the lncRNA-mediated ceRNA regulatory mechanisms underlying the effects of TG in the treatment of AD.

Keywords: Alzheimer's disease, tripterygium glycoside, competitive endogenous RNA, microarray

Correspondence: Jianming Li
Department of Basic Biology, Changsha Medical College, Changsha, People's Republic of China
Tel +86 731-88528679
Email ljming0901@sina.com

Introduction

Alzheimer's disease is the most common type of dementia, accounting for approximately 50%-70% of the total cases of dementia.[1] The typical pathological features of AD include senile plaques formed by the overproduction and aggregation of amyloid β (Aβ) and neuronal fiber tangles formed by intracellular

hyperphosphorylated tau protein.[2] A number of current hypotheses about the pathogenesis of AD cannot completely explain the disease.[3] The existing treatment of AD is inconclusive or invalid. Investigation of new drugs or methods is required to treat the symptoms of AD. Tripterygium glycoside (TG) is extracted from the roots of *Tripterygium wilfordii* Hook.f, and has been shown to protect against rheumatoid arthritis (RA),[4] lupus nephritis (LN),[5] diabetes mellitus (DM),[6] and Guillain-Barre syndrome (GBS).[7] Animal experiments showed that TG has protective effects on the central nervous system.[8,9] Wang et al suggested that TG can significantly improve the inflammatory damage of astrocytes induced by lipopolysaccharides (LPS).[10] Additionally, Wang et al reported that anti-inflammatory effects of TG are mediated by enhanced expression of IL-37.[11] However, the molecular mechanism of action of TG in the treatment of $A\beta_{25-35}$-induced AD in mice were not investigated.

Competing endogenous RNAs (ceRNAs) are closely associated with the development of neurodegenerative diseases. The ceRNA hypothesis was initially proposed by Salmena et al in 2011.[12] The hypothesis proposed that various RNA molecules, such as messenger RNAs (mRNAs) and long noncoding RNAs (lncRNAs), are involved in the competitive binding or sharing of microRNAs (MREs). Thus, the effect of miRNAs on the target genes can be removed or reduced to influence human development and related diseases,[13] which are closely associated with aging, apoptosis, and cell fate.

The CeR mechanism was shown to be involved in the pathogenesis of AD. High expression of BACE1 neurons is a key factor in the production of Aβ.[14] LncRNA BACE1-AS is the antisense noncoding transcript of BACE1 mRNA, which can increase the expression of BACE1 mRNA.[15,16] Subsequent studies have shown that miR-29, miR-107, miR-124, and miR-485 can bind to BACE1 mRNA and BACE1-AS.[16] BACE1 mRNA and BACE1-AS may play a role as competing ceRNAs. Nuclear enriched transcriptase 1 (NEAT1) is a lncRNA detected in mammalian cells, is elevated in Aβ-treated SH-SY5Y cells, and aggravates Aβ-induced neuronal injury through miR-107.[17] NEAT1 was also significantly upregulated in an AD mouse model. Inhibition of NEAT1 or overexpression of NEAT1 can upregulate or downregulate the expression of miR-124, respectively, to influence the expression of BACE1.[18] Furthermore, cyclin-dependent kinase 5 activating factor 1 (CDK5R1) is closely associated with the genesis and development of AD.[19] Three lncRNAs, including NEAT1, Hox transcriptional antisense RNA, and metastasis-associated lung adenocarcinoma transcriptome 1, can positively regulate the miR-15/107 family, and the miR-15/107 family can decrease the expression of CDK5R1 by modifying the stability of its mRNA[20] However, the lncRNA-miRNA-mRNA regulatory networks were not investigated in an AD mouse model treated with TG.

In the present study, we aimed to investigate the expression profiles of lncRNAs, miRNAs, and mRNAs and construct a lncRNA-related ceRNA network in $A\beta_{25-35}$-induced AD mouse model treated with TG. In addition, functional enrichment analyses and a protein-protein interaction (PPI) network were performed to reveal the underlying mechanism of TG in the treating AD.

Materials and Methods

AD Mouse Model and Study Design

The protocols of these animals were followed the National Institutes of Health Guide for the Care and Use of Laboratory Animals. The research protocol was approved by the Ethics Committee of Changsha Medical University, China (EC20190114). Sixty-four C57BL/6J mice (male, 25.1 ± 5.4 g, 7 months of age) were obtained from Hunan Tianqin Biotechnology Co., Ltd. (Changsha, Hunan, China). In the AD mouse model group, 32 C57BL/6J mice were administered 3 μL of $A\beta_{25-35}$ (dual side, 1 mg/mL) by a single stereotactic injection in the brain (bromega: 2.3mm, lambda: 1.8mm, depth: 2.0mm). In the control group, 32 C57BL/6J mice were administered 3 μL of normal saline (dual side, 1 mg/mL) by a single stereotactic injection in the brain. A total of 32 AD mice were randomly selected and divided into two groups: the AD+normal saline (NS) group (n=16) and the AD +TG group (n=16). Mice in the AD+TG group were treated with TG (0.25mg/10g.d, 1mg/mL) by intraperitoneal injection and lasted for 4 weeks. TG (10mg/tablet) was obtained in the form of tablets (TG tablets) from Fujian Huitian Bio-pharma Co., Ltd. (GMP certificated, Fujian, China). The dosing and duration of TG followed the study conducted by Wang et al.[21] Mice in the AD+NS group were treated with normal saline (0.9%) (0.5mL/d) by intraperitoneal injection and lasted for 4 weeks. Alterations in the spatial learning and memory deficits in the AD+NS and AD+TG groups were detected by the Morris water maze test as described by Vorhees et al.[22]

The expression of p-tau and $A\beta_{25-35}$ proteins was evaluated by immunohistochemistry.

Sample Collection

The mice were anaesthetized with pentobarbital sodium (0.2%, 0.1 mL/10 g) by intraperitoneal injection. Eight samples of the brain tissue from each group were stored in 10% neutral formalin, and other samples were stored at −80°C (n=8).

Immunohistochemistry

Paraffin sections of the tissues were baked for 2 hours until dewaxing in water and incubated in 3% hydrogen peroxide solution for 10 min at room temperature in the dark. BSA (5%) was added for 20 min, and 50 μL of mouse anti-p-tau or anti-$A\beta_{25-35}$ antibodies (1:400; Chemicon, USA) were added at 4°C overnight. Then, the tissues were reacted with 50 μL of anti-mouse immunoglobulin G (IgG) (1:500; Chemicon, USA) at 37°C for 50 min and incubated with the avidin-biotin reagents (1:500; Burlingame, CA, USA). The immunoreactive product was visualized in 0.003%H2O2 and 0.05% 3, 3′-diaminobenzidine. The results were detected by light microscope.

RNA Extraction

An E.Z.N.A.® total RNA kit II (Omega, USA) was used to isolate total RNA from hippocampus tissue samples. A NanoDrop ND-2000 (Thermo Scientific) was used to quantify the total RNA. An Agilent Bioanalyzer 2100 (Agilent Technologies) was used to assess the RNA integrity (RIN) of the total RNA.

Microarray Analysis

A total of 6 animal RNAs (AD+NS vs AD+TG: 3:3) were used for microarray analysis. An Agilent mouse lncRNA microarray (4*180K, design ID:085631) and an Agilent mouse miRNA microarray (8x60K, design ID:070155) were used to detect the differentially expressed lncRNAs, miRNAs, and mRNAs. The microarray experiments were performed by OEBiotech Corporation (Shanghai, China). Sample labeling, microarray hybridization, and washing were performed according to the standard protocols.

Identification of Differentially Expressed Genes

The array images were analyzed by Feature Extraction software (version 10.7.1.1, Agilent Technologies). The basic analysis of the raw data was performed by Genespring (version 14.8, Agilent Technologies). The raw data were normalized according to the quantile algorithm. The fold changes (FC) and P values based on a *t*-test were used to identify differentially expressed lncRNAs, mRNAs, and miRNAs. A FC≥ 2.0 ($P < 0.05$) were set as the thresholds for up- and downregulated genes. Target genes of differentially expressed miRNAs were predicted using the miRDB and miRWalk databases. The differentially expressed patterns of lncRNAs, mRNAs, and miRNAs in the samples were analyzed by hierarchical clustering.

Quantitative Real-Time-PCR (qRT-PCR) and Statistical Analysis

A HiScript 1st strand cDNA synthesis kit (#R312-01, Beyotime, Beijing, China) was used to synthesize cDNA. SYBR™ Select master mix (#Q221-01, Beyotime, Beijing, China) was used for qRT-PCR. The Ct values were analyzed by SDS software 2.0 (PE Biosystem, ABI, USA). The relative expression levels of differentially expressed lncRNAs, mRNAs, and miRNAs were analyzed using the $2^{-\Delta\Delta Ct}$ method and normalized to β-actin. SPSS (version 19.0, SPSS, Inc., Chicago, IL, USA) was used to perform the statistical tests.

ceRNA Network Analysis

Pearson's r was used to calculate the correlations between miRNA and mRNA, miRNA and lncRNA, and mRNA and lncRNA in 6 samples with the threshold value for the correlation coefficient ≥ 0.80 ($P < 0.05$). The MuTaME method was used to calculate the ceRNA score for the relationship pairs with a predicted regulatory relationship, and the P value of the corresponding ceRNA relationship was calculated according to the hypergeometric distribution.

Functional Annotation

Gene ontology (GO) and Kyoto Encyclopedia of Genes and Genomes (KEGG) analyses were used to determine the potential biological functions and pathways of differentially expressed mRNAs by the Database for Annotation Visualization and Integrated Discovery (DAVID) tool (https://david.ncifcrf.gov/).

Construction of the Protein-Protein Interaction (PPI) Network

To identify the potential relationships of differentially expressed mRNAs, a protein-protein interaction (PPI) network based on the top 50 upregulated and downregulated

mRNAs was constructed by using STRING (v10.5, https://string-db.org/cgi/input.pl) and visualized by Cytoscape 3.6.1.

Results

The Effect of TG on an $A\beta_{25-35}$-Induced AD Mouse Model

The results of the Morris water maze test showed that the AD mouse model group had significantly longer latency ($p<0.05$) and swimming distances and a lower frequency of traveling into the quadrant with the hidden platform than the normal control group ($p < 0.05$) (Figure 1A, B, D, E). And the AD +TG mouse model group had significantly shorter latency ($p<0.05$) and swimming distances and a higher frequency of traveling into the quadrant with the hidden platform than the AD+NS mouse model group ($p < 0.05$)(Figure 1C-E). The relative mean density of Aβ marker densities were significantly lower in the AD+TG group compared to those in the AD mouse model group ($p<0.05$) (Figure 1F-I). The amount of p-Tau protein integral optical density (IODs) were significantly lower in the AD+TG group compared to those in the AD+NS group ($p<0.05$)(Figure 1J-M).

Differentially Expressed lncRNA, mRNA, and miRNA

A total of 503 differentially expressed(DE) mRNAs (422 upregulated and 81 downregulated), 661 DElncRNAs (341 upregulated and 320 downregulated), and 13 DEmiRNAs (7 upregulated and 6 downregulated) were detected based on the threshold of FC≥ 2.0 ($P < 0.05$). The volcano maps and heat maps of the clustering analysis of RNAs are shown in Figure 2.

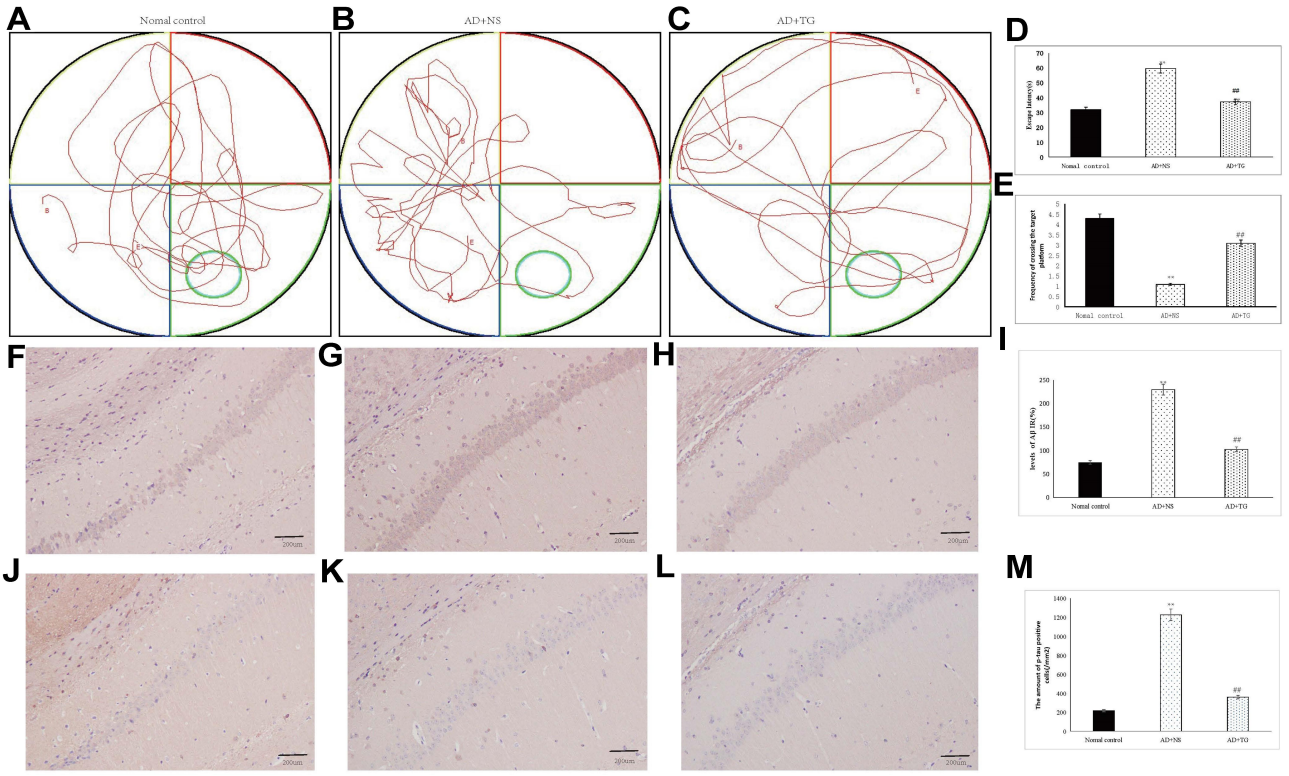

Figure 1 The effect of TG in Aβ25-35-induced AD mouse model. (**A**) Swimming trajectory in Normal control group by Morris water maze. (**B**) Swimming trajectory in AD +NS group by Morris water maze. (**C**) Swimming trajectory in AD+TG group by Morris water maze. (**D**) Significant difference of escape latency in the AD+TG group than that in the AD+NS group was detected (**, Normal control group vs AD+NS group, $p<0.05$; ##, AD+TG group vs AD+NS group, $p<0.05$). € Significant more frequency of crossing the target platform in AD+TG group than that in the AD+NS group was detected (**, Normal control group vs AD+NS group, $p<0.05$; ##, AD+TG group vs AD +NS group, $p<0.05$). (**F**) Light microscopic images show the distribution of Aβ immunolabeling across the brain of Normal control group (40X). (**G**) Light microscopic images show the distribution of Aβ immunolabeling across the brain of AD+NS group (40X). (**H**) Light microscopic images show the distribution of Aβ immunolabeling across the brain of AD+TG group (40X). (**I**) The comparison of relative mean density of Aβ marker densities in AD+NS and AD+TG groups. The images revealed that the relative mean density of Aβ is higher in the AD+NS group than those in the AD+TG group. (n = 16/group in the AD+TG group; n = 16/group in the AD+TG group)(**, Normal control group vs AD+NS group, $p<0.05$; ##, AD+TG group vs AD+NS group, $p<0.05$). (**J**) Light microscopic images show the distribution of p-Tau immunolabeling across the brain of Normal control group (40X). (**K**) Light microscopic images show the distribution of p-Tau immunolabeling across the brain of AD+NS group (40X). (**L**) Light microscopic images show the distribution of p-Tau immunolabeling across the brain of AD+TG group (40X). (**M**) The comparison of p-Tau positive neurons in AD+NS and AD+TG groups. The images revealed that the p-Tau expressed higher in the AD+NS group than those in the AD+TG group. (n = 16/group in the AD+TG group; n = 16/group in the AD+TG group)(**, Normal control group vs AD+NS group, $p<0.05$; ##, AD+TG group vs AD+NS group, $p<0.05$).TG: Tripterygium glycoside; AD: Alzheimer disease; NS: normal saline.

CeRNA Network in an $A\beta_{25-35}$-Induced AD Mouse Model Treated with TG

The DEmRNA-DEmiRNA-DElncRNA pairs were arranged according to the ceRNA scores. The ceRNA network involving the top 200 DEmRNA-DEmiRNA-DElncRNA pairs with 16 DElncRNAs, 11 DEmiRNAs, and 52 DEmRNAs was visualized using Cytoscape software and is shown in Figure 3.

Functional Analysis of DEmRNAs in the ceRNA Network

Functional analysis revealed that 503 DEmRNAs in the ceRNA network were enriched in 188 GO biological process, 15 cellular_component, and 51 molecular_function categories. The most enriched GO term in the biological process (BP) category was "cellular response to ethanol"; the most enriched GO term in the cellular component category was "external side of plasma membrane"; the most enriched GO term in the molecular function category was "transcriptional activator activity, RNA polymerase II proximal promoter sequence-specific DNA binding" (Figure 4A and Table 1).

The KEGG pathway analysis identified a total of 14 significantly enriched pathways. "Staphylococcus aureus infection", "PI3K-Akt signaling pathway", and "ECM-receptor interaction" were the top 3 significantly enriched terms (Figure 4B and Table 2).

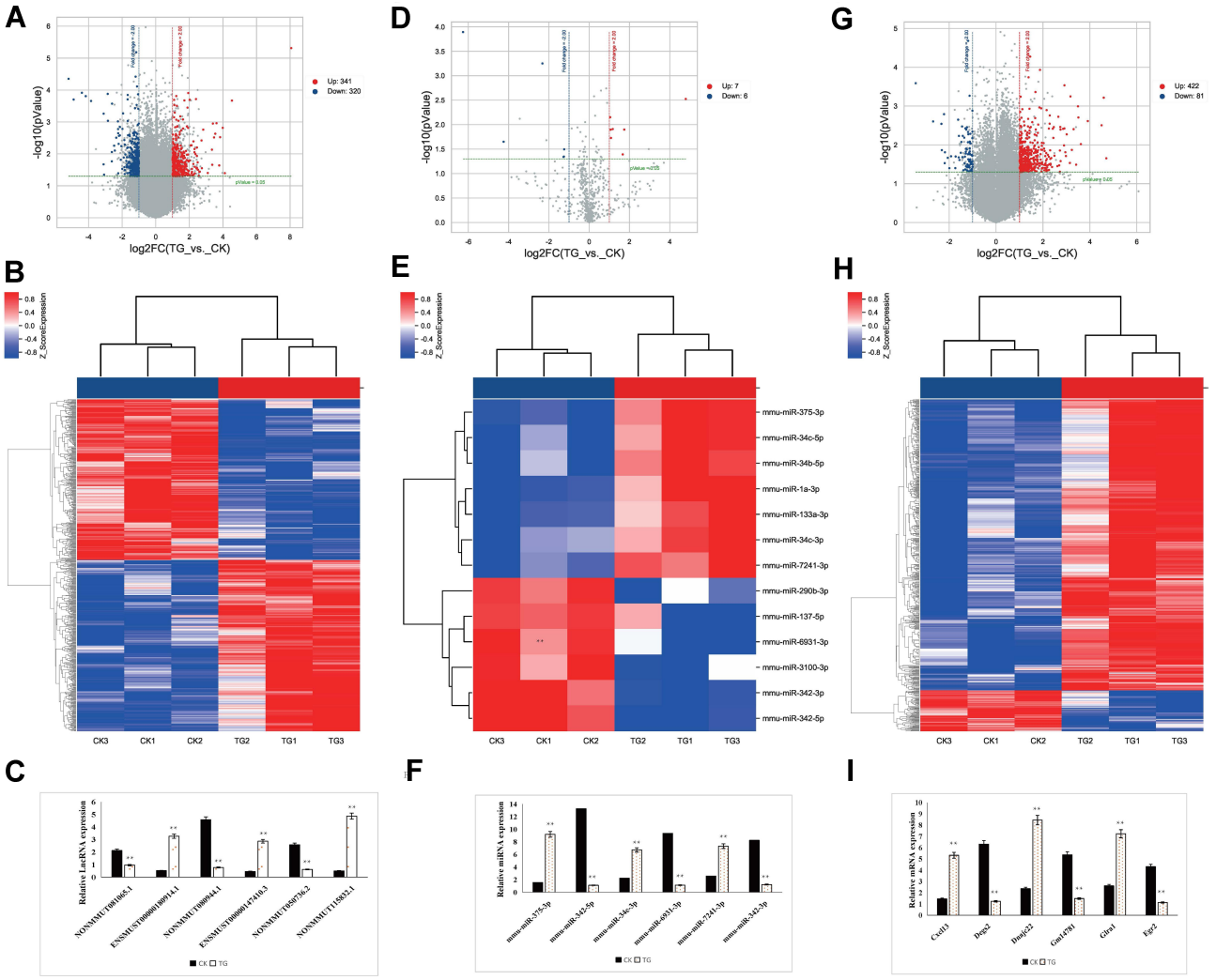

Figure 2 The expression profiles of lncRNAs, mRNAs, and miRNAs between AD models and AD models treated with Tripterygium glycoside (TG). (**A**) Volcano plot of differentially expressed lncRNAs, (**B**) Heatmap of differentially expressed lncRNAs; (**C**) Relative expression of lncRNAs. The quantitative real-time PCR (qRT-PCR) validated 6 randomly selected lncRNAs. The results were consistent with the microarray data. (**D**) Volcano plot of differentially expressed miRNAs. (**E**) Heatmap of differentially expressed miRNAs; (**F**) Relative expression of miRNAs. The qRT-PCR validated 6 randomly selected miRNAs. The results were consistent with the microarray data. (**G**) Volcano plot of differentially expressed mRNAs. (**H**) Heatmap of differentially expressed RNAs between AD models and AD models treated with Tripterygium glycoside (TG). (**I**) Relative expression of mRNAs. The qRT-PCR validated 6 randomly selected mRNAs. The results were consistent with the microarray data. **, AD+TG vs AD+NS group, $p<0.05$. CK: AD+NS; TG: AD+TG.

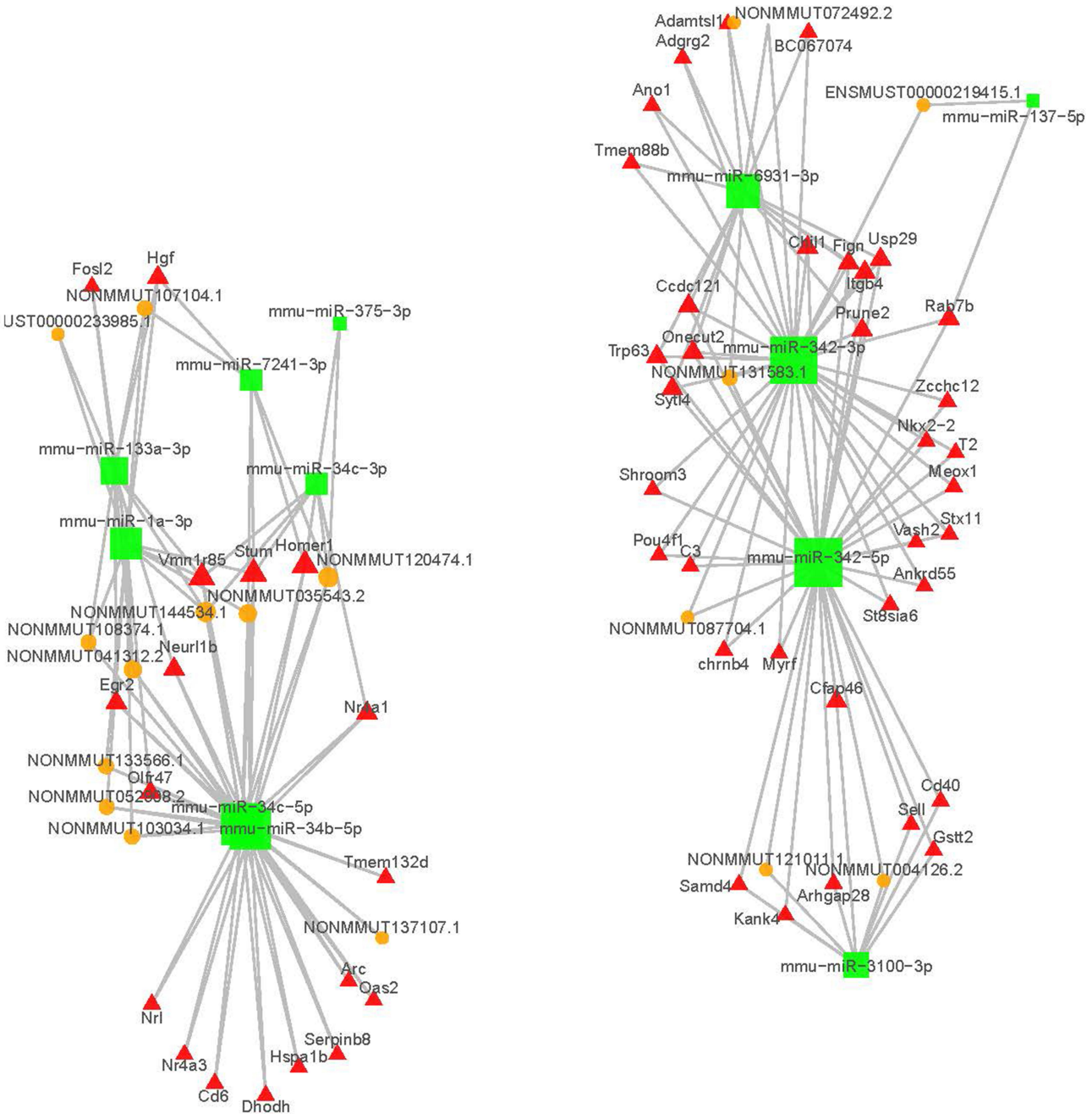

Figure 3 The top 200 lncRNA-miRNA-mRNA ceRNA network. The red rectangles indicate mRNAs, green square represent miRNAs and orange circles represent lncRNAs.

Protein-Protein Interaction (PPI) Network

As shown in Figure 4C, the top 50 DEmRNAs were identified in the PPI network including 26 nodes and 19 edges. Seven most significant hub genes including C3, CXCL13, Plac8, Egr1, Egr2, Egr4, and Pou4f1 had more interactions with other proteins.

Discussion

Alzheimer's disease is a common neurodegeneration disease charactered by progressive cognitive impairment and behavioral impairment driving pathologenesis. The mechanism is complex and not clear yet. And there is no effective treatment for this disease. TG, also known as tripterygium, is the total glycosides extracted from the

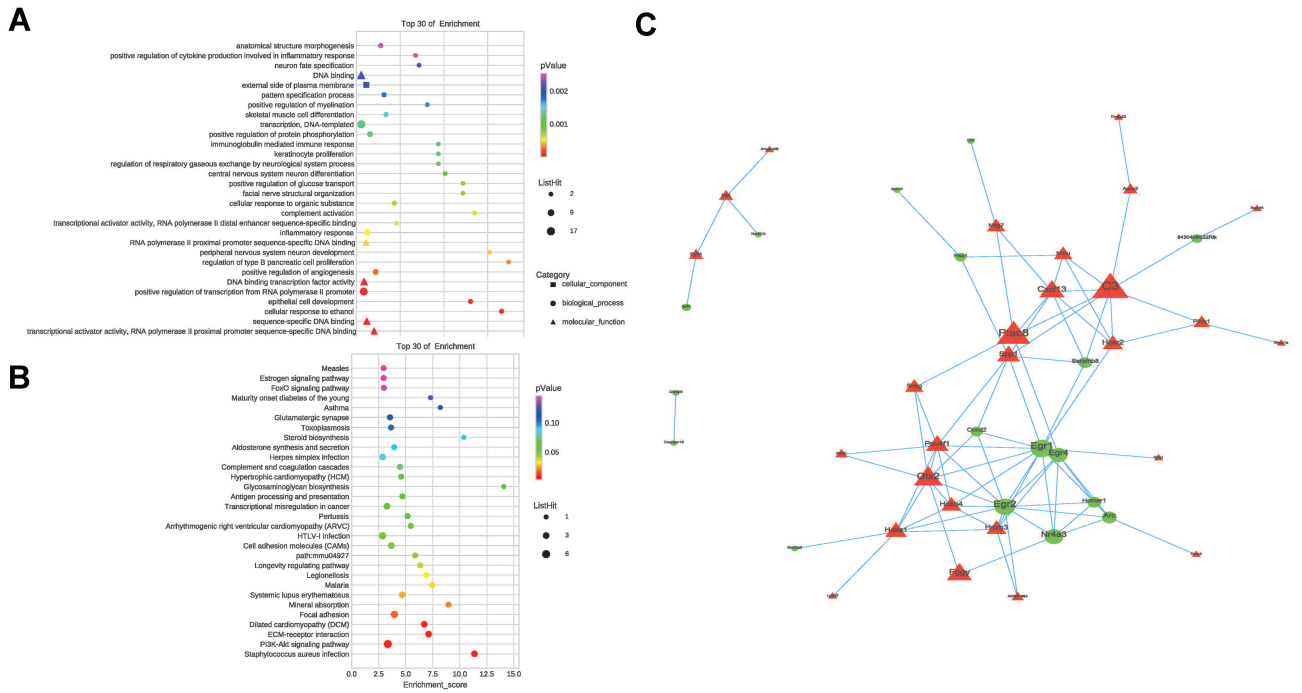

Figure 4 Functional analysis of DEmRNAs in the ceRNA network. (**A**)Top 30 enriched GO pathway of DEmRNAs involved in the ceRNA network. (**B**) Top 30 enriched KEGG pathway of DEmRNAs involved in the ceRNA network. (**C**) Protein regulation network analysis. The protein-protein interaction networks were constructed by Cytoscape Software. Proteins are represented with color nodes, and interactions are represented with edges. Red and green represent up-regulation and down-regulation.

peeled roots of *Tripterygium wilfordii Hook.f.* has protective effects on the central nervous system in animal experiments.[9,11] Our study demonstrated that TG can significantly improve spatial memory and inhibit the production of p-tau in an $A\beta_{25\text{-}35}$-induced AD mouse model, indicating that TG had anti-inflammatory and neuroprotective effects.

Currently, most effort has been made to elucidate the roles of ncRNAs involved in the pathologenesis and prognosis of AD.[23–28] The ceRNA hypothesis suggested a new mechanism for RNA interaction.[29] MiRNA activity is an important factor in the posttranscriptional regulation and can be regulated by lncRNAs through "sponge" adsorption.[30] LncRNAs act as ceRNAs to competitively bind to miRNAs to influence miRNA-induced gene silencing, regulating the protein levels and participating in the regulation of the expression of the target genes. Zhang et al demonstrated that MAGI2-AS3 acts as competing endogenous RNA or a molecular sponge in negatively modulating miR-374b-5p by targeting BACE1 on Aβ-induced neurotoxicity and neuroinflammation.[31] In addition, three lncRNA AP000265.1, KB-1460A1.5 and RP11-145M9.4 were also identified to regulating the neurofibrillary tangles by sponging miRNAs such as miR-20a, miR-17-5p and miR-106b in AD.[32] Furthermore, Ma et al have identified 487, 89, and 3,025 significantly dysregulated lncRNAs, miRNAs, and mRNAs and conducted comprehensive lncRNA-associated ceRNA networks in the APP/PS1 mice brain. This role of CeR regulation mechanism might provide a novel prediction and therapeutic target for AD.[33]

To investigate the potential mechanism of action of ncRNAs in the treatment of AD with TG, we identified DElncRNAs, DEmRNAs, and DEmiRNAs and successfully constructed a lncRNA-associated ceRNA network in an AD mouse model treated with TG. In the present study, we detected 661 DElncRNAs (341 upregulated and 320 downregulated) in an $A\beta_{25\text{-}35}$-induced AD mouse model treated with TG. Among the DElncRNAs, NONMMUG090228.1 was the most upregulated lncRNA with an FC of 268.27. NONMMUG011123.2 was the most downregulated lncRNA with an FC of 36.50. Notably, larger number of lncRNAs have been identified in animal models and human patients with AD. Zhou et al found 24 up-regulated and 84 down-regulated lncRNAs in AD patients. And the up-regulated lncRNA n336934 was shown to be linked to cholesterol homeostasis.[34] Cao et al reported that the expressions of age-associated lncRNAs-SNHG19 and LINC00672, were significantly correlated with Braak stage of AD.[35] Moreover, in our previous study, we successfully generated an intranasal

Table 1 The Top Five Gene Ontology Analysis of DEmRNAs Associated with Alzheimer's Disease Mice Models Treated with Tripterygium Glycoside

Term_ID	Term_Description	ListHit	ListTotal	PopHit	PopTotal	GeneRatio	BgRatio	Enrichment_Score	GeneIds	GeneSymbols	P_value	FDR_bh	Category
GO:0071361	Cellular response to ethanol	3	83	11	20,209	0.036144578	0.000544312	66.4041621	14,654;15,394;11,513	Glra1;Hoxa1;Adcy7	1.08E-05	0.005747855	Biological_process
GO:0002064	Epithelial cell development	3	83	14	20,209	0.036144578	0.000692761	52.1746988	27,428;22,061;225,631	Shroom3;Trp63;Onecut2	2.35E-05	0.006169857	Biological_process
GO:0045944	Positive regulation of transcription from RNA polymerase II promoter	15	83	1094	20,209	0.180722892	0.054134297	3.338417656	15,370;13,654;225,631;22,061;18,516;21,939;18,124;15,394;18,996;13,653;18,088;14,284;17,285;15,223;18,185	Nr4a1;Egr2;Onecut2;Trp63;Pbx3;Cd40;Nr4a3;Hoxa1;Pou4f1;Egr1;Nkx2-2;Fosl2;Meox1;Foxj1;Nr1	3.47E-05	0.006169857	Biological_process
GO:0045766	Positive regulation of angiogenesis	5	83	138	20,209	0.060240964	0.006828641	8.821808975	15,234;226,841;12,266;21,939;12,654	Hgf;Vash2;C3;Cd40;Chil1	0.000261522	0.034913158	Biological_process
GO:0061469	Regulation of type B pancreatic cell proliferation	2	83	7	20,209	0.024096386	0.00034638	69.56626506	15,370;18,124	Nr4a1;Nr4a3	0.000345331	0.035636702	Biological_process

LPS-mediated AD mouse model and identified a total of 395 lncRNAs that are potentially associated with the pathogenesis of AD.[36] However, the relationships of NONMMUG011123.2 and NONMMUG090228.1 with AD were not investigated previously. Therefore, it is necessary to investigate the functions of these two lncRNAs in AD treated with TG in the future.

However, having identified several specific lncRNAs for $A\beta_{25-35}$-induced AD mouse treated with TG, the present study drew a comprehensive ceRNA network, which revealed the complexity of the regulatory relationships among DElncRNAs, DEmiRNAs and DEmRNAs. The immunoinflammatory response induced by Aβ deposition in the brain is one of the important pathological mechanisms of AD. Activation of the complement system is involved in the immune inflammatory response in the brain of AD. C1q is the promoter of the classical complement activation pathway, C3 is the intersection of the classical complement activation pathway, the bypassing pathway and the lectin pathway. Aβ can bind with C1q and C3 to activate the complement system, respectively, and cause the complement cascade reaction.[37] Increased C3 mRNA expression in the frontal cortex of AD patients has been reported.[38] Furthermore, TG could significantly inhibited the expression of C3 in the cortex of AD rat models.[39] Our results demonstrated that lower expression of C3 in $A\beta_{25-35}$-induced AD mouse treated with TG compared with AD models, which strongly suggested its role in the pathologenesis of AD. The ceRNA network predicted that C3 was a target gene of miR-342-5p and miR-342-3p. Sun et al demonstrated that the expression of miR-342-5p was significantly increased in APP/PS1, PS1ΔE9, and PS1-M146V transgenic mice. Upregulated miR-342-5p leads to downregulated expression of ankyrin G (AnkG), which results in abnormal AIS filtering function of hippocampal neurons in AD transgenic mice, including loss of selectivity for macromolecules entering the axons.[40] Moreover, enhanced magnetic resonance imaging of amyloid plaques in AD was positively correlated with the expression of the serum marker miR-342-3p in amyloidosis.[41] Serum miR-342-3p expression was significantly increased after treatment with Yam pills in the AD group compared to that at baseline.[42] Our data shown decreased expression of miR-342-5p and miR-342-3p was detected in $A\beta_{25-35}$-induced AD mouse treated with TG. Bioinformatic analysis predicted that miR-342-5p and miR-342-3p may both interact with NONMMUT087704.1 or NONMMUT131583.1, the increased expression of

Table 2 The Top Five KEGG Analysis of DEmRNAs Associated with Alzheimer's Disease Mice Models Treated with Tripterygium Glycoside

Term_ID	Term_Description	ListHit	ListTotal	PopHit	PopTotal	GeneRatio	BgRatio	Enrichment_Score	GeneIds	GeneSymbols	P_value	FDR_bh	Classification_LevelI
path: mmu05150	Staphylococcus aureus infection	3	40	52	7874	0.075	0.006604013	11.35673077	12,268;211,924;12,266	C4b;Dsg1c;C3	0.002259289	0.286929655	Human Diseases
path: mmu04151	PI3K-Akt signaling pathway	6	40	353	7874	0.15	0.04483109	3.345892351	15,370;15,234;192,897;245,026;16,420;27,219	Nr4a1;Hgf;Itgb4;Col6a6;Itgb6;Sgk2	0.008210125	0.314038811	Environmental Information Processing
path: mmu04512	ECM-receptor interaction	3	40	83	7874	0.075	0.010541021	7.115060241	192,897;245,026;16,420	Itgb4;Col6a6;Itgb6	0.008427397	0.314038811	Environmental Information Processing
path: mmu05414	Dilated cardiomyopathy (DCM)	3	40	88	7874	0.075	0.011176022	6.710795455	192,897;16,420;11,513	Itgb4;Itgb6;Adcy7	0.009890986	0.314038811	Human Diseases
path: mmu04510	Focal adhesion	4	40	199	7874	0.1	0.025273051	3.95678392	192,897;15,234;245,026;16,420	Itgb4;Hgf;Col6a6;Itgb6	0.017782988	0.440470363	Cellular Processes

which was also positively correlated with the pathogenesis of AD treated with TG. Although the function of NONMMUT087704.1 and NONMMUT131583.1 is poorly annotated, it is conceivable that NONMMUT087704.1 and NONMMUT131583.1 may act as a ceRNA to interact with miR-342-5p or miR-342-3p by targeting C3 in AD.

GO analysis revealed that DEmRNAs were enriched in 188 biological processes. Significant GO terms involved "peripheral nervous system neuron development", "central nervous system neuron differentiation", and "neuron fate specification". Pathway analysis demonstrated that 14 pathways were enriched and were primarily involved in "PI3K-Akt signaling pathway" and "cell adhesion molecule (CAM) signaling pathway". The PI3K/Akt signaling pathway is one of the classical signaling pathways in the regulation of apoptosis and plays an important role in the occurrence, development, and treatment of AD and other neurodegenerative diseases.[43] Activation of the PI3K/Akt signaling pathway can protect neurons from Aβ-induced neurotoxicity, and inhibition of Akt phosphorylation can aggravate cognitive and memory impairment in patients with AD.[44] Moreover, the PI3K/Akt signaling pathway can mediate the neuroprotective effects of phytoestrogens and Chinese herbal preparations.[45] We generated a PPI network based on the top 50 key DEmRNAs to elucidate the mechanisms of action of the ceRNA network. Most of DEmRNAs in the PPI network, including C3, CXCL13, Plac8, Egr1, Egr2, Egr4, and Pou4f1, were shown to be closely associated with inflammation, plasticity of neurons, and learning and memory processes of central neurons.[46,47]

Conclusions

In the present study we identified 503 DEGs, 661 DElncRNAs, and 13 DEmiRNAs during treated with TG in $A\beta_{25-35}$-induced AD mouse model. And we firstly constructed a lncRNA-miRNA-mRNA ceRNA network based on the DElncRNAs, DEmRNAs, and DEmiRNAs and filtered 26 gene nodes in DEGs to construct a PPI network complex. The results may provide novel insight into the mechanisms of ceRNA regulation in an $A\beta_{25-35}$-induced AD mouse model treated with TG.

Funding

The present study was funded by the National Natural Science Foundation of China (Grant No. 81873780, 61702054); Hunan Natural Science Foundation Youth Program (2019JJ50697, 2018JJ3568); The Changsha

Outstanding Innovative Young People Training Scheme (kq2009095, kq2009093, kq2004077); The Foundation of the Education Department of Hunan Province (19A058, 19B072); The Foundation of Health and Family Planning Commission of Hunan Province (20201918, 20201910); The Foundation of the Education Department of Guangxi Province (2021KY1959); The Application Characteristic Discipline of Hunan Province; The Hunan Key Laboratory Cultivation Base of the Research and Development of Novel Pharmaceutical Preparations (No. 2016TP1029).

Disclosure

The authors declare no conflicts of interest.

References

1. Bai MK, Ammu R, Shee PN, et al. Current concepts of neurodegenerative mechanisms in alzheimer's disease. *BioMed Res Int*. 2018;2018:1–12.
2. Kim MS, Kim Y, Choi H. Transfer of a healthy microbiota reduces amyloid and tau pathology in an Alzheimer's disease animal model. *Gut*. 2019;69:317431.
3. Tol J, Roks G, Slooter A, et al. Genetic and environmental factors in alzheimer's disease. *Rev Neurol*. 1999;155:S10.
4. Bu X, Fan J, Hu X, et al. Norwegian scabies in a patient treated with Tripterygium glycoside for rheumatoid arthritis. *An Bras Dermatol*. 2017;92(4):556–558.
5. Lian F, Wang Y, Xu H, et al. Chinese experience with tripterygium wilfordii multiglycoside as long-term maintenance therapy in lupus nephritis. *An Rheu Dis*. 2013;71:675.2–675.
6. Liu JH, Li Y, Huang LY. Effects of insulin on intervention therapy of Tripterygium Polyglycoside combine with Nicotinamide in LADA patients. *Chin J Modern Med*. 2005;15:145–147.
7. Zhang X, Xia J, Ye H. Effect of Tripterygium polyglycoside on interleukin-6 in patients with Guillain-Barre syndrome. *Zhongguo Zhong XI Yi Jie He Za Zhi*. 2000;20(5):332–334.
8. Frisoni GB, Boccardi M, Barkhof F. Strategic roadmap for an early diagnosis of Alzheimer's disease based on biomarkers. *Lancet Neurol*. 2017;16:661–676.
9. Jiang Q, Tang XP, Chen XC. Will Chinese externaltherapy with compound Tripterygium wilfordii hook F gel safely control disease activity in patients with rheumatoidarthritis: design of adouble-blinded randomized controlled trial. *BMC Complement Altern Med*. 2017;17:444.
10. Wang M, Chen TG, Yang XL. Effect of tripterygium glycosides on inflammatory factors induced by lipopolysaccharide in rat astrocytes. *Chin J Clin Pharmacol*. 2019;35:154–158.
11. Wang S, Li R, He S. Tripterygii Radix et Rhizoma glycosides upregulate the new anti-inflammatory cytokine IL-37 through ERK1/2 and p38 MAPK signal pathways. *Evid Based Complement Alternat Med*. 2017;2017:9148523.
12. Salmena L, Poliseno L, Tay Y, et al. A cerna hypothesis: the rosetta stone of a hidden rna language? *Cell*. 2011;146(3):353–358.
13. Tay Y, Rinn J, Pandolfi PP. The multilayered complexity of ceRNA crosstalk and competition. *Nature*. 2014;505:344–352.
14. Bera S, Santiago EC, Barca C, et al. Ap reduces amyloidogenesis by promoting bace 1 trafficking and degradation in neurons. *EMBO Rep*. 2020;21(e47954):1–21.
15. Liu T, Huang Y, Chen JL, et al. Attenuated ability of BACE1 to cleave the amyloid precursor protein via silencing long noncoding RNA BACE1-AS expression. *Mol Med Rep*. 2014;10:1275.
16. Fotuhi SN, Khalaj-Kondori M, Feizi MAH, et al. Long non-coding rna bace1-as may serve as an alzheimer's disease blood-based biomarker. *J Mol Neurosci*. 2019;69:351–359.
17. Ke S, Yang Z, Yang F, et al. Long noncoding rna neat1 aggravates aβ-induced neuronal damage by targeting mir-107 in alzheimer's disease. *Yonsei Med J*. 2019;60:640.
18. Zhao MY, Wang GQ, Wang NN, et al. The long-non-coding RNA NEAT1 is a novel target for Alzheimer's disease progression via miR-124/BACE1 axis. *Neurol Res*. 2019;41:489–497.
19. Marco S, Barbara G, Francesco R, et al. Multiple layers of cdk5r1 regulation in alzheimer's disease implicate long non-coding rnas. *Int J Mol Sci*. 2018;19:2022.
20. Moncini S, Lunghi M, Valmadre A. The mir-15/107 family of microrna genes regulates cdk5r1/p35 with implications for alzheimer's disease pathogenesis. *Mol Neurobiol*. 2017;54:4329–4342.
21. Wang M, Chen TG, Yang XL. Effect of tripterygium glycosides on inflammatory factors induced by lipopolysaccharide in rat astrocytes. *Chin J Clinical Pharmacol*. 2019;35:154–158.
22. Vorhees CV, Williams MT. Morris water maze: procedures for assessing spatial and related forms of learning and memory. *Nature Protocol*. 2006;1:848–858.
23. Faghihi MA, Modarresi F, Khalil AM, et al. Expression of a noncoding RNA is elevated in Alzheimer' s disease and drives rapid feed-forward regulation of β-secretase expression. *Nat Med*. 2008;14:723–730.
24. Ciarlo E, Massone S, Penna I, et al. An intronic ncRNA-dependent regulation of SORL1 expression affecting Aβ formation is upregulated in post-mortem Alzheimer's disease brain samples. *Dis Model Mech*. 2013;6:424–433.
25. Massone S, Vassallo I, Fiorino G, et al. 17A, a novel non-coding RNA, regulates GABA B alternative splicing and signaling in response to inflammatory stimuli and in Alzheimer disease. *Neurobiol Dis*. 2011;41:308–317.
26. Massone S, Ciarlo E, Vella S, et al. NDM29, a RNA polymerase III-dependent non coding RNA, promotes amyloidogenic processing of APP and amyloid beta secretion. *Biochim Biophys Acta*. 2012;1823:1170–1177.
27. Mus E, Hof PR, Tiedge H. Dendritic BC200 RNA in aging and in Alzheimer's disease. *Proc Natl Acad Sci U S A*. 2007;104:10679–10684.
28. Parenti R, Paratore S, Torrisi A, et al. A natural antisense transcript against Rad18, specifically expressed in neurons and upregulated during beta-amyloid-induced apoptosis. *Eur J Neurosci*. 2007;26:2444–2457.
29. Zhang T, Huang W. Modelling competing endogenous RNA networks. *J Cancer Ther*. 2015;06:622–630.
30. Thomson DW, Dinger ME. Endogenous microRNA sponges: evidence and controversy. *Nat Rev Genet*. 2016;17:272–283.
31. Zhang J, Wang R. Deregulated lncRNA MAGI2-AS3 in Alzheimer's disease attenuates amyloid-βinduced neurotoxicity and neuroinflammation by sponging miR-374b-5p. *Exper Gerontol*. 2020;144.
32. Wang LK, Chen XF, He DD, Li Y, Fu J. Dissection of functional lncRNAs in Alzheimer's disease by construction and analysis of lncRNA-mRNA networks based on competitive endogenous RNAs. *Biochem Bioph Res Co*. 2017;3:569–576.
33. Ma N, Tie C, Yu B, Zhang W, Wan J. Identifying lncRNA–miRNA–mRNA networks to investigate Alzheimer's disease pathogenesis and therapy strategy. *Aging (Albany NY)*. 2020;12(3):1–24.
34. Zhou X, Jie X. Identification of Alzheimer's disease–associated long noncoding RNAs. *Neurobiol Aging*. 2015;36(11):2925–2931.
35. Cao M, Li H, Zhao J, Cui J, Hu GK. Identification of age- and gender-associated long noncoding RNAs in the human brain with Alzheimer's disease. *Neurobiol Aging*. 2019;81:116–126.
36. Tang L, Liu L, Li GY, Jiang PC, Wang Y, Jm L. Expression profiles of long non-coding RNAs in intranasal LPS-mediated Alzheimer's disease model in mice. *Biomed Res Int*. 2019;9642589.

37. Yu JX, Bradt BM, Hsiao K, Cooper NR. C3 is associated with amyloid plaques in the transgenic mouse model of Alzheimer's disease. *Mol Immunol*. 1998;35(6):337.
38. Fischer B, Schmoll H, Platt D, Popa-Wagner A, Riederer P, Bauer J. Complement C1q and C3 mRNA expression in the frontal cortex of Alzheimer's patients. *J Mol Med*. 1995;73(9):465–471.
39. Cheng L, Hu XL, Yang BL. Effects of triptolide on the expressions of C1q and C3 after microinjection of beta-amyloid protein into cerebral cortex in rats. *Chin J Gerontol*. 2011;31:800–803.
40. Sun X, Wu Y, Gu M, et al. miR-342-5p Decreases Ankyrin G Levels in Alzheimer's Disease Transgenic Mouse Models. *Cell Rep*. 2014;6:264–270.
41. Zhang YZ, Cao QY, Yang HL. Correlation between contrast enhanced MRI and serum markers of amyloidosis in patients with Alzheimer's disease. *Shandong Arch Psychi*. 2018;31:446–449.
42. Xie WT, Tan ZH, Chen Y, et al. Effect of modified Yam Pills on serum specific MicroRNAs expression in patients with mild and moderate Alzheimer's disease. *J Nanjing Univer Trad Chin Med*. 2018;34:485–490.
43. Satoru M, Yukie N, Ai T, et al. Implications of PI3K/AKT/PTEN signaling on superoxide dismutases expression and in the pathogenesis of Alzheimer's disease. *Diseases*. 2018;6:E28.
44. Fatemeh S, Fereshteh M, Fariba K. Inhibition of Akt phosphorylation diminishes mitochondrial biogenesis regulators, tricarboxylic acid cycle activity and exacerbates recognition memory deficit in rat model of Alzheimer's disease. *Cell Mol Neurobiol*. 2014;34:1223–1233.
45. Meng XB, Wang M, Sun GB, et al. Attenuation of Aβ 25-35-induced parallel autophagic and apoptotic cell death by gypenoside XVII through the estrogen receptordependent activation of Nrf2/ARE pathways. *Toxicol Appl Pharm*. 2014;279:63–75.
46. Krumbholz M, Theil D, Cepok S, et al. Chemokines in multiple sclerosis: CXCL12 and CXCL13 up-regulation is differentially linked to CNS immune cell recruitment. *Digest World Core Med J*. 2006;129:200–211.
47. Wei F, Xu ZC, Qu ZC, et al. Role of Egr1 in Hippocampal synaptic enhancement induced by tetanic stimulation and amputation. *J Cell Biol*. 2000;149:1325–1334.